Results in Physics 76 (2025) 108378

Contents lists available at ScienceDirect

Results in Physics

journal homepage: www.elsevier.com/locate/rinp

Ion-selective membrane-integrated water-gated AlGaN/GaN HEMT for high-stability detection of agricultural herbicides

Amirul Firdaus [a], Najihah Fauzi [a], Shuhadah Ismail [b], Nur Atiqah Hamzah [a], Rashidah Shukor [d], Hiroshi Kawarada [c,e], Shaili Falina [b,c,*], Mohd Syamsul [a,c,*]

[a] Institute of Nano Optoelectronics Research and Technology (INOR), Universiti Sains Malaysia, 11800 Pulau, Pinang, Malaysia
[b] Collaborative Microelectronic Design Excellence Centre (CEDEC), Engineering Campus, Universiti Sains Malaysia, 11800 Pulau, Pinang, Malaysia
[c] Faculty of Science and Engineering and Institute of Nano Science and Nano Engineering, Waseda University, Tokyo 169-8555 Shinjuku, Japan
[d] Department of Food Science, Faculty of Food Science and Technology, Universiti Putra Malaysia, 43400 Serdang, Selangor, Malaysia
[e] Power Diamond Systems Inc, Tokyo 169-0051 Shinjuku, Japan

ARTICLE INFO

Keywords:
HEMT
FET
Sensor
WGHEMT
Herbicide

ABSTRACT

This research work presents the development and characterization of a water-gated high electron mobility transistor (WGHEMT) sensor for real-time detection of herbicides, specifically glyphosate, paraquat, and diquat. Conventional FET-based sensors often suffer from design rigidity, as they are not modular and typically require complex fabrication steps for each specific target analyte. These limitations hinder their reusability for practical environmental monitoring applications. The WGHEMT utilizes a dual-pool electrolyte-gating mechanism with a replaceable ion-selective membrane (ISM) to modulate charge interactions at the AlGaN/GaN interface. Electrical and potentiometric responses were evaluated for both stock and commercial formulations, revealing that WGHEMT performance is highly dependent on herbicide concentrations. Paraquat consistently demonstrated the highest sensitivity due to its dicationic structure, while commercial glyphosate showed enhanced performance, attributed to improved ionic mobility from surfactants. Current sensitivity reached up to 761.029 μA/mg L^{-1} for commercial paraquat with excellent linearity (R^2 = 0.96173). The WGHEMT exhibited strong stability and repeatability, with drift values under 1 % during time-dependent measurements for all herbicides concentrations. The WGHEMT adopts a modular approach through its interchangeable ISM, allowing flexible detection of various herbicides without requiring structural modifications. These results highlight the WGHEMT sensor's high sensitivity, reliability, and suitability for field-based herbicide monitoring, underscoring the importance of calibrating WGHEMTs with commercial formulations for accurate environmental assessment.

Introduction

The widespread use of herbicides in modern agriculture has significantly enhanced crop yields and food security, yet their extensive application has led to persistent environmental contamination and growing public health concerns [1]. Among the most commonly used herbicides, glyphosate, paraquat, and diquat are particularly problematic due to their chemical stability, mobility in water systems, and well-documented toxicological effects [2]. Farmers, who are in direct and frequent contact with these herbicides, face heightened exposure risks, making them particularly vulnerable to the harmful effects of these chemicals. Glyphosate, a broad-spectrum systemic herbicide, is the most heavily used agrochemical worldwide, with annual global consumption exceeding 800,000 metric tons [3]. Despite its effectiveness, glyphosate and its primary metabolite aminomethylphosphonic acid (AMPA) have been detected in various water sources, raising concerns about long-term ecological and human health impacts [4]. The International Agency for Research on Cancer (IARC, 2015) classified glyphosate as a Group 2A probable human carcinogen, further intensifying regulatory scrutiny. Paraquat and diquat, both highly toxic compounds, are known for their acute lethality and association with fatal poisoning cases [5]. Paraquat in particular generates reactive oxygen species that cause severe oxidative damage in biological systems [6].

Current methods for herbicide detection, such as chromatography

* Corresponding authors at: Institute of Nano Optoelectronics Research and Technology (INOR) and Collaborative Microelectronic Design Excellence Centre (CEDEC), Universiti Sains Malaysia, 11800 Pulau Pinang, Malaysia
E-mail addresses: shailifalina@usm.my (S. Falina), nasyriq@usm.my (M. Syamsul).

https://doi.org/10.1016/j.rinp.2025.108378
Received 6 June 2025; Received in revised form 15 July 2025; Accepted 28 July 2025
Available online 28 July 2025

and immunoassays offer high sensitivity but suffer from major limitations including high operational costs, complex sample preparation, and the need for sophisticated laboratory infrastructure [11–13]. These constraints have created an urgent need for rapid, cost-effective, and field-deployable sensing technologies capable of real-time herbicide monitoring in water sources. Recent advancements in semiconductor-based biosensors have opened new possibilities for environmental pollutant detection, with field-effect transistor (FET)-based sensors gaining prominence due to their label-free operation, high sensitivity, and compatibility with miniaturized systems [14]. A particularly promising development is the water-gated FET (WGFET), which utilizes an aqueous electrolyte as the gate dielectric, enabling ultra-low voltage operation and high sensitivity to surface charge variations [15]. WGFET differ from traditional FETs by replacing the solid dielectric with an aqueous electrolyte, enabling the formation of an electric double layer (EDL) at the electrolyte–semiconductor interface. This EDL provides ultra-efficient gating, resulting in higher sensitivity to surface charge changes compared to conventional FET [16]. Unlike traditional FET, WGFET offer direct interaction with analytes, enabling real-time, label-free sensing in liquid environments.

In recent years, sensors based on AlGaN/GaN high electron mobility transistor (HEMT) structures have garnered significant attention owing to their exceptional material characteristics. These advantages stem primarily from the presence of a high-density two-dimensional electron gas (2DEG), elevated saturation velocity linked to superior carrier mobility, and their inherently wide band gap [17,18]. The formation of the 2DEG is driven by spontaneous and piezoelectric polarization effects, both of which are essential for enabling efficient electron transport within the AlGaN/GaN heterojunction. This high electron mobility is frequently used as a benchmark for evaluating the quality of epitaxial layers, thereby contributing to the enhanced performance of the sensor, particularly in herbicide detection applications [19]. Furthermore, the proximity of high-density 2DEG channels to the surface renders the device highly responsive to surface ion variations, supporting fast and accurate detection across a diverse range of chemical targets [20].

Water-gated high electron mobility transistors (WGHEMT) represent a further evolution of this technology, combining the benefits of high carrier mobility materials with the advantages of aqueous-phase sensing [21]. The unique properties of AlGaN/GaN HEMT enhance sensitivity while ensuring long-term reliability in aqueous environments [22]. Moreover, by functionalizing the ion selective membrane (ISM) surface with specific recognition elements, selective detection of target herbicides can be achieved without direct modification of the semiconductor channel [23]. In a dual-pool water-gated configuration, the incorporation of an ISM is essential. The ISM serves as the key sensing interface, enabling specific ion recognition and effective modulation of the channel conductivity. Without the ISM, the system lacks the necessary functionality to operate as a true water-gated structure. Building on a similar approach, Kerstin et al. and collaborators pioneered the development of a functional water-gated sensor utilizing an organic field-effect transistor (OFET) for the selective detection of sodium (Na^+) and potassium ions (K^+). In their design, a polyvinyl chloride-based ion-selective membrane (PVC-ISM) was used as the sensing membrane [24]. The operational principle of this sensor is rooted in potentiometry, wherein the potential difference is measured between the transducing electrode (OFET) and a reference electrode (Ag/AgCl). Potentiometric sensors are known for their advantages, including fast response times, user-friendly design, cost-effectiveness, and robustness against turbidity interference [25]. Similarly, Alqahtani et al. introduced a water-gated sensing platform that employed conductive oxide-based thin-film transistors (SnO_2 TFTs) as the transducer, also using PVC as the ISM. Their system demonstrated favourable performance in terms of sensitivity, selectivity, and recovery time for detecting a range of ions, including K^+, Na^+, Cs^+, Cu^{2+}, Pb^{2+}, F^-, and Hg^{2+} [26,27]. These foundational studies highlight the versatility and potential of water-gated sensor platforms for ion detection. Nevertheless, further research is warranted to explore additional performance parameters beyond sensitivity, selectivity, and recovery characteristics.

Despite advances in WGHEMT-based sensing, existing herbicide detection platforms lack modularity, leading to fabrication complexity and limited reusability [28]. To address this challenge, this study presents a modular sensor system that incorporates an interchangeable ion-selective membrane (ISM), enabling the HEMT device to be easily reused for multiple herbicide targets while simplifying the overall fabrication process. Our approach integrates high-sensitivity transistors with a reusable, interchangeable sensing membrane and microfluidic sample handling. By optimizing device architecture and surface functionalization, we achieve detection limits below regulatory thresholds (e.g., 0.1 μg/L for glyphosate as per EPA guidelines), offering a scalable, cost-effective alternative to conventional methods. For all measurements, a single HEMT transducer was used to detect all three herbicides, making the approach cost-effective. By simply replacing the ISM, the same HEMT could be reused without degradation by separate HEMT and herbicide solution for each herbicide. Notably, the WGHEMT exhibits high sensitivity and stability due to the dual-pool configuration. The success of this technology could revolutionize herbicide detection, providing a critical tool for regulatory compliance, agricultural runoff management, and drinking water safety. The research work demonstrates the first application of this transistor platform for herbicide detection while overcoming the stability and degradation issues of conventional systems. The modular and interchangeable ISM design allows flexible herbicide detection, providing proof-of-concept validation for its adaptability and highlighting its potential for integration into portable environmental monitoring systems for real-world applications.

Experimental methods

WGHEMT growth, fabrication and measurement

The AlGaN/GaN heterostructures were grown epitaxially on sapphire substrates via metal–organic chemical vapor deposition (MOCVD) using a horizontal-flow reactor (Taiyo Nippon Sanso Corporation, SR4000KS-HT). The GaN layer was developed through a two-step process, beginning with a 20 nm GaN buffer layer, followed by a 1.2 μm-thick primary GaN layer and a subsequent 2.2 μm-thick GaN layer. A 22 nm-thick AlGaN layer containing 25 % aluminium was then deposited. The fabricated devices measured 5 mm × 5 mm. Ohmic contacts at the source and drain were established through electron beam deposition of a Ti/Al/Ni/Au metal stack (20 nm/160 nm/55 nm/45 nm), followed by rapid thermal annealing (RTP) at 860 °C for 60 s in a nitrogen (N_2) atmosphere to enhance contact quality. The resulting transducer was mounted on a glass substrate, with electrical connections affixed to the source and drain terminals and securely fastened. The ion-sensitive membrane (ISM) was formed by depositing a 2 nm-thick gold (Au) or silver (Ag) film onto a 280 μm-thick, single-side polished p-type silicon wafer using electron beam deposition. To form the AuNis or AgNis sensing layer, the surface underwent RTP at 400 °C for 60 s. The surface morphology of the fabricated ISM layers was then characterized using field emission scanning electron microscopy (FESEM).

The WGHEMT structure was developed using AutoCAD software and fabricated with a Photon Mono 4 K resin-based 3D printer, as shown in Fig. 1. The design comprises three main components: a reference pool, an herbicide pool, and a dedicated housing chamber for the ISM. In potentiometric sensing, the voltage differential between the two pools is critical. The reference pool contains a stable reference solution that maintains a constant potential, while the herbicide pool holds the test solution, where the applied bias (V_{HP}) is influenced by the concentration of target ions. The HEMT transducer, reference electrode, and ISM are positioned in the reference pool, herbicide pool, and ISM chamber, respectively. Each pool includes a 2 cm-diameter aperture facing the ISM housing to facilitate ion exchange. The ISM functions as a selective membrane that permits targeted ionic transport while physically

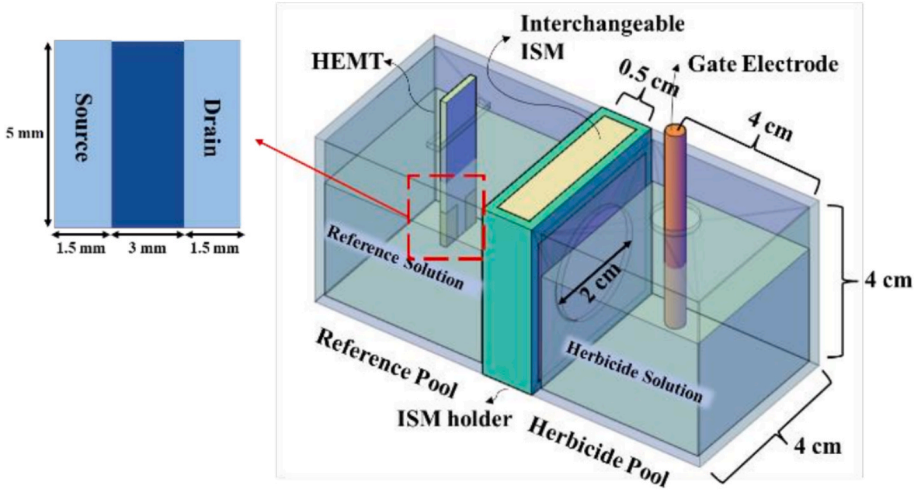

Fig. 1. WGHEMT configuration.

isolating the solutions in each pool. Additionally, the ISM housing incorporates 2 cm ports on both sides to enable controlled diffusion of ions without compromising spatial separation. This configuration allows the HEMT transducer and reference electrode to function within their respective environments, while ion transfer across the ISM modulates the effective bias (V_{EF}) enabling accurate sensing of the target analyte [29].

Device connectivity was achieved by bonding conductive wires to the source and drain terminals using conductive epoxy. To ensure electrical insulation and mechanical protection, the HEMT transducer was encapsulated in epoxy resin, with a precisely defined area of the AlGaN surface deliberately left uncovered to enable interaction with the target analyte and maintain the sensor's functionality. The WGHEMT was exposed to test using various pH solutions and herbicides such as stock glyphosate (PESTANAL®, analytical standard), stock paraquat (PESTANAL®, analytical standard), stock diquat (PESTANAL®, analytical standard), commercial used glyphosate (ECOMAX) and commercial used paraquat (Syngenta). Commercial diquat could not be tested, as it has recently been banned in Malaysia and is no longer available on the market. For pH solutions, a 1 × PBS solution with an initial pH of 7.4 was modified to the desired pH levels by gradually adding 0.1 mol/L HCl for acidic adjustments or 0.1 mol/L KOH for basic adjustments. Throughout the process, the solution was continuously stirred, and the pH was monitored in real time using a pH meter (Hanna Instruments) until the target pH was achieved. This process was redo for each required pH level.

To stabilize the herbicide stock solution, it was diluted at pH 5.5, as herbicide exhibits greater chemical stability at this mildly acidic pH [30]. A phosphate buffer was used for the dilution process. A 1 × PBS solution with an initial pH of 7.4 was adjusted to the desired pH levels by gradually adding 0.1 mol/L hydrochloric acid (HCl). The solutions were continuously stirred, and the pH was monitored in real time using a pH meter (Hanna Instruments) until the target pH was achieved. Subsequently, the solution was serially diluted using the prepared buffer to obtain concentrations of 0.01, 0.1, 1, 10, and 100 (mg L^{-1}). Each dilution step was performed by transferring a fixed volume of the previous solution into a new container and diluting it tenfold, ensuring consistency and accuracy across all concentration levels. The same dilution procedure was applied to the commercially available herbicides. Notably, chemical isolation of the active compounds in commercial herbicide formulations was intentionally omitted. This decision was made to evaluate the WGHEMT sensor's sensitivity in the presence of additional ingredients typically found in real-world agricultural formulations, thereby better simulating practical sensing conditions. The selected concentrations reflect realistic herbicide usage levels, which are typically around 5.3 mg/L in actual field applications [3]. The value of 5.3 was selected as it lies in the middle of the response range, allowing the sensor to detect both tenfold lower and higher concentrations, thus offering a wider detection range.

Electrical characterization was performed by immersing the HEMT transducer in the reference pool containing a pH 7 reference solution, while a platinum electrode was positioned in the herbicide pool filled with target solutions at concentrations ranging from 0.001 to 10 (mg mL^{-1}). The WGHEMT's drain and source terminals were connected to the corresponding ports of a Keithley 2400 Semiconductor Device Analyzer (SMU). Additionally, the platinum electrode was connected to the gate terminal of the SMU to enable gate bias modulation throughout the measurement process. The output (I_D–V_D) and transfer (I_D–V_G) characteristics were measured under varying herbicide concentrations by applying a constant gate voltage (V_G) of −1 V and a constant drain voltage (V_D) of 1 V respectively. Time-resolved measurements were subsequently conducted by monitoring the drain current (I_D) at a fixed V_D of 0.5 V over a period of 240 s. To reduce cross-contamination between measurements, the platinum reference electrode was rinsed with deionized (DI) water for 10 s after each test. Prior to data acquisition, the reference electrode was immersed in the target solution and allowed to stabilize for 60 s. All measurements were performed at room temperature using a gate bias voltage (V_G) ranging from −1.5 V to −7.5 V, which was applied to the solution via the reference electrode under a constant WGHEMT bias of 1 V. The working voltage of a HEMT refers to the optimal range of gate and drain voltages applied to ensure stable, efficient transistor operation without causing leakage or breakdown. In the case of WGHEMTs, a gate voltage between −1.5 V and −7.5 V is generally optimal for achieving consistent and efficient performance. For glyphosate detection, the ISM employed in the WGHEMT sensor consists of AuNis on p-Si, based on the work of Guan et al. who demonstrated effective glyphosate sensing using gold nanoparticles-based interfaces [31]. For paraquat detection, the WGHEMT utilizes AgNis as the ISM on p-Si, following the approach reported by Ali et al. and Hu et al. where silver nanoparticles were successfully applied for paraquat and diquat detection [32,33].

These configurations leverage the strong electrochemical interactions between the respective nanoparticles and target analytes, thereby enhancing the WGHEMT's sensitivity and selectivity. The overall dimensions of the WGHEMT have been considered to evaluate its practical applicability. Each water-gated pool, including both the sensing and reference compartments, measures 4 × 4 × 4 cm. While the current design is intended for benchtop measurements and proof-of-concept validation, the compact form factor suggests potential for further miniaturization. Inclusion of these physical dimensions allows a

more comprehensive assessment of the WGHEMT's portability and suitability for future field-deployable implementations. The WGHEMT sensor configuration was shown in Fig. 1.

To investigate the influence of the 2DEG in the presence WGHEMT structures, both low and high concentration of herbicides were modeled and simulated using the Victory Device simulator on SILVACO TCAD. The simulation incorporated multiple physical models, including the Shockley–Read–Hall (SRH) model to account for carrier recombination via defect states within the semiconductor. Polarization effects were included to induce 2DEG formation along the heterojunction channel. Additionally, the Newton iteration method was utilized for simulating trap-assisted recombination, while the numerical solver facilitated the modeling of carrier transport, capturing both electron and hole dynamics. Ohmic contacts were assigned to the source and drain terminals, whereas the gate and AuNis/AgNis structures were treated as Schottky contacts with a work function of 5.15 eV. Each AuNis/AgNis element on the p-Si surface was modeled individually to resemble its actual nanoscale structure, without forming ohmic contacts. The simulation framework was specifically developed to examine the 2DEG concentration at low and high herbicide concentrations.

The model was specifically designed to investigate the effects of AuNis/AgNis modification on the p-Si surface. To isolate this effect, the AlGaN layer was set to a thickness of 22 nm, while the substrate and buffer layers were intentionally omitted. The source–drain distance was defined as 18 μm. This simplified configuration enabled a more focused analysis of the impact of both low and high herbicide concentrations on the AlGaN surface behavior. For the reference solution, germanium (Ge) was selected as the representative material due to its similarity to an electrolyte with electrically neutral charge distribution and a relative permittivity (ε) of 80, corresponding to that of water ($\varepsilon_w = 80$). To model the herbicide pool, two concentration conditions were considered: low and high. For the low herbicide concentration, Ge doped at 1×10^{14} cm^{-3} was used, while for the high concentration, heavily doped Ge at 1×10^{19} cm^{-3} was selected.

Results and discussion

Sensing mechanism

The sensing mechanism of the water-gated high electron mobility transistor (WGHEMT) is governed by the formation of an EDL at the interfaces of both the reference and herbicide pools. This interfacial behaviour is described by the conventional Gouy–Chapman–Stern (GCS) model, which represents the EDL equilibrium at the metal–solution interface [34]. The inclusion of p-type silicon (p-Si) in the system facilitates complementary operation by enhancing the performance of the n-type HEMT transducer [35]. The mechanism begins with EDL formation at the electrode surface, as described by the Stern model, which assumes purely electrostatic interactions between the charged electrode surface and the surrounding ions, without involving any faradaic (electron transfer) reactions. These electrostatic forces originate from charge accumulation or depletion at the electrode surface, creating a potential difference relative to the solution. This potential is neutralized by an opposing layer of counterions, leading to the formation of a characteristic two-layered charge structure known as the electric double layer [36]. When a bias is applied to the electrode, positively or negatively charged, solvent molecules and ions organize themselves into two distinct regions: the inner Helmholtz plane (IHP), where solvent molecules and specifically adsorbed anions align, and the outer Helmholtz plane (OHP), where loosely bound counterions accumulate to balance the surface charge. Schmoltner et al. have noted that the water-gated sensing mechanism is driven by the V_{EF}, which comprises both the membrane potential and the externally applied V_G. In terms of surface electrostatics, the V_{EF} of the WGHEMT herbicide sensor can be interpreted as the surface potential of the AlGaN layer, $\varphi_{surface\ (AlGaN)}$, which is determined by the sum of the total surface potential, φ_{sum}, and the potential drop across the Stern layer (also referred to as the screening potential), $\varphi_{scr\ (AlGaN)}$, as expressed in Eq. (1). This relationship is adapted from Varghese et al., who analysed the behaviour of the Stern layer on semiconductor surfaces [37].

$$V_{EF} = \varphi_{surface\ (AlGaN)} = \varphi_{sum} - \varphi_{scr\ (AlGaN)} \tag{1}$$

To evaluate φ_{sum} influencing $\varphi_{surface\ (AlGaN)}$, the contribution from surface potential at Si, $\varphi_{surface\ (Si)}$, p-Si, $\varphi_{surface\ (p\text{-}Si)}$, and electrode, $\varphi_{surface\ (el)}$ are deemed.

$$\varphi_{sum} = \varphi_{surface\ (Si)} + \varphi_{surface\ (p\text{-}Si)} + \varphi_{surface\ (el)} \tag{2}$$

The Eq. (2) can be substitute into Eq. (1) to calculate V_{EF} as equated in Eq. (3).

$$\varphi_{surface\ (AlGaN)} = [\varphi_{surface\ (Si)} + \varphi_{surface\ (p\text{-}Si)} + \varphi_{surface\ (el)}] - \varphi_{scr\ (AlGaN)} \tag{3}$$

Based on Eq. (1), the surface potentials at Si, p-Si, and the electrode are derived and then substituted into Eq. (3) to obtain Eq. (4).

$$\begin{aligned}\varphi_{surface\ (AlGaN)} = [&(\varphi_{reference\ pool\ solution} - \varphi_{scr\ (Si)}) \\ &+ (\varphi_{herbicide\ pool\ solution} - \varphi_{scr\ (p\text{-}Si)}) \\ &+ (\varphi_{herbicide\ pool\ solution} - \varphi_{scr\ (el)})] - \varphi_{scr\ (AlGaN)}\end{aligned} \tag{4}$$

The φ_{scr} for all surfaces including AlGaN, Si, p-Si and electrode can be expressed by Eq. (5).

$$\varphi_{scr} = \frac{\sigma_{dl}}{C_{Stern}} \tag{5}$$

where the ratio of surface charge density due to diffusion (σ_{DL}) and capacitance of the Stern layer (C_{Stern}). The $\varphi_{solution}$ for the reference pool and herbicide pool is evaluated as Eq. (6).

$$\varphi_{solution} = \sigma_{solution} \times \frac{E}{Q} \tag{6}$$

Here, *E* denotes the permissible energy level within the crystal lattice of GaN and Si in the absence of an external electric field, with its value determined by the crystal structure and charge carrier transport mechanisms of the respective materials. The term *Q* refers to the elementary charge. The interface charge is defined in Eq. (7).

$$\sigma_{solution} = Q_{pH} \times C_{pH} \times N_A \tag{7}$$

The electrical potentials of the references and herbicide pool solutions are determined by the surface charge density, Q_{pH}, and the ionic concentration of the respective solutions, C_{pH}, with N_A representing Avogadro's constant. The I_D is modulated by changes in the two-dimensional electron gas (2DEG) density, $\Delta\eta s$, which are induced by variations in the surface potential, as described in Eq. (8).

$$\Delta\eta_s = \frac{\epsilon_{AlGaN}}{d_{eff}} \left(\frac{d_{2DEG}}{d_{eff}} \varphi_{surface\ (AlGaN)}\right) \tag{8}$$

In this context, $\varepsilon_{(AlGaN)}$ denotes the permittivity of the AlGaN layer, d_{2DEG} represents the spatial separation between the 2DEG and the heterointerface, while d_{eff} refers to the effective distance between the sensing gate and the 2DEG channel. Consequently, a reduction in the V_{EF} leads to a corresponding decrease in the I_D, and vice versa.

Paraquat and diquat are redox-active bipyridinium herbicides that exist as stable dications across all pH conditions, owing to their quaternized nitrogen atoms. Paraquat (1,1′-dimethyl-4,4′-bipyridinium) and diquat (1,1′-ethylene-2,2′-bipyridinium) exhibit high aqueous solubility and interact strongly with negatively charged interfaces due to their permanent + 2 charge. These properties enable efficient detection via potentiometric or electrochemical transducers functionalized with anionic surface groups such as carboxylates. Glyphosate exhibits a zwitterionic structure in aqueous environments, with its charge state varying depending on pH [38]. It contains both positively charged amino groups and negatively charged phosphonate and carboxylic

groups. At low pH, glyphosate becomes predominantly positively charged due to the protonation of amino groups [39]. However, our findings suggest that under the experimental conditions used—particularly in the specific buffer composition and WGHEMT configuration—glyphosate exhibits behaviour consistent with a net positive charge. This observation aligns with reports that the speciation of glyphosate can shift depending on local pH, ionic strength, and complexation with metal ions (e.g., Ca^{2+}, Fe^{3+}), which may result in positively charged complexes or dominant cationic interactions [40].

This observation suggests that at high herbicide concentrations, the reduced presence of anions results in fewer cations being attracted to the electrode's OHP as illustrated in Fig. 2. In the EDL diffusion region, both anions and cations are limited, including those attracted to the AuNis or AgNis/p-Si ISM [41]. To maintain charge neutrality in the herbicide pool, a small number of cations accumulate at the OHP of the AuNis or AgNis/p-Si interface. This causes a slight repulsion of holes from the p-Si into the undoped Si region, which in turn draws in electrons. Consequently, fewer holes remain near the undoped Si surface connected to the reference pool, attracting a limited amount of anions to the OHP. The overall low ionic concentration at the ISM OHP results in a reduced φ_{sum}, thereby lowering V_{EF}. Likewise, in the reference pool, relatively few anions are drawn to the undoped Si, and lower number of cations are attracted to the AlGaN surface. To balance the charge of the reference pool, only a small number of cations are present at the AlGaN OHP. This limited ionic attraction leads to a low-density 2DEG and thus a decreased I_D under high concentration of herbicides conditions, consistent with prior results.

In contrast, at low herbicide concentrations, the WGHEMT sensing mechanism under a +1 V bias is depicted in the Fig. 3. The elevated number of anions in the solution promotes greater cation accumulation at the electrode's OHP. In the electrode's EDL diffusion zone, anion migration toward the electrode is minimal, and the attraction of cations to the AuNis or AgNis/p-Si ISM is similarly constrained. Nevertheless, to preserve charge neutrality within the herbicide pool, a higher concentration of cations accumulates at theOHP near the AuNis or AgNis/p-Si interface. This results in a significant displacement of holes from the p-Si region into the adjacent undoped Si, thereby promoting electron attraction from the undoped Si. As a result, hole accumulation increases at the undoped Si surface facing the reference pool, which in turn draws more anions to the corresponding OHP. The resulting increase in both cation and anion concentration in the ISM's OHP leads to a higher φ_{sum} and, therefore, an elevated V_{EF}. Similarly, within the EDL of the reference pool, limited anion attraction to the undoped Si coincides with a low presence of cations at the AlGaN interface. To balance the reference pool charge, a significant number of cations accumulate at the AlGaN OHP. Ultimately, the low herbicide concentration promotes high-density 2DEG formation, thereby enhancing I_D [31].

Fig. 4a present a comparison of electron concentration (cm^{-3}) between the low and high concentration of herbicide, highlighting an enhancement in carrier density within the 2DEG channel upon WGHEMT. The electron concentration for the bare high concentration is approximately 3.46×10^{19} cm^{-3}, while the low concentration exhibits a higher concentration of about 5.26×10^{19} cm^{-3}. In a similar trend, Fig. 4b illustrates the electron current density (A/cm^2), which also decrease with the presence of herbicide. The high concentration records a current density of roughly 10.61 MA/cm^2, compared to approximately 16.36 $\times$ MA/cm^2 for the AuNis-modified device. These results confirm that the 2DEG properties are attributed to the concentration of the herbicides.

Surface characterization of AuNis and AgNis ISM

The surface morphology of AuNis and AgNis was characterized using FESEM. As shown in Figs. 4 and 5a, the top-view FESEM image of AuNis reveals uniformly distributed, densely packed gold nanostructured islands with an average diameter ranging from 6 to 29 nm. Similarly, Fig. 5b presents the top-view FESEM image of AgNis, exhibiting a comparable uniform and dense distribution of nanostructured islands with diameters ranging from 7 to 30 nm. The formation of nanostructured islands leads to a substantial increase in surface area, which in turn improves the sensitivity and performance of sensing applications [42].

WGHEMT pH detection

pH detection can be an effective approach to assess the performance of WGHEMT as a reliable sensor. Fig. 6a presents the output current (I_D-V_D) characteristics, measured at a fixed V_G of 1 V across pH values ranging from 2 to 12. A progressive increase in I_D values was observed with increasing pH, indicating the device's sensitivity to changes in ionic concentration. As the pH increases, the amount of anions in the solution increases, preceding to a higher accumulation of counterions at the OHP. In the EDL diffusion region, the distribution of ions adjusts according to lower concentrations of anions and cations are attracted to the electrode and the AuNis/p-Si ISM, respectively. Simultaneously, more cations are drawn toward the OHP at the AuNis/p-Si ISM to

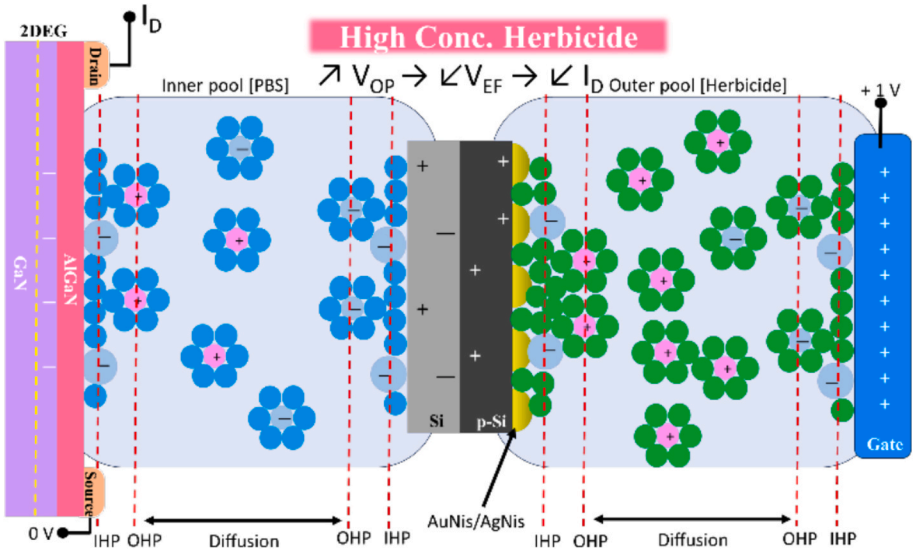

Fig. 2. WGHEMT sensing mechanism in high concentration herbicides.

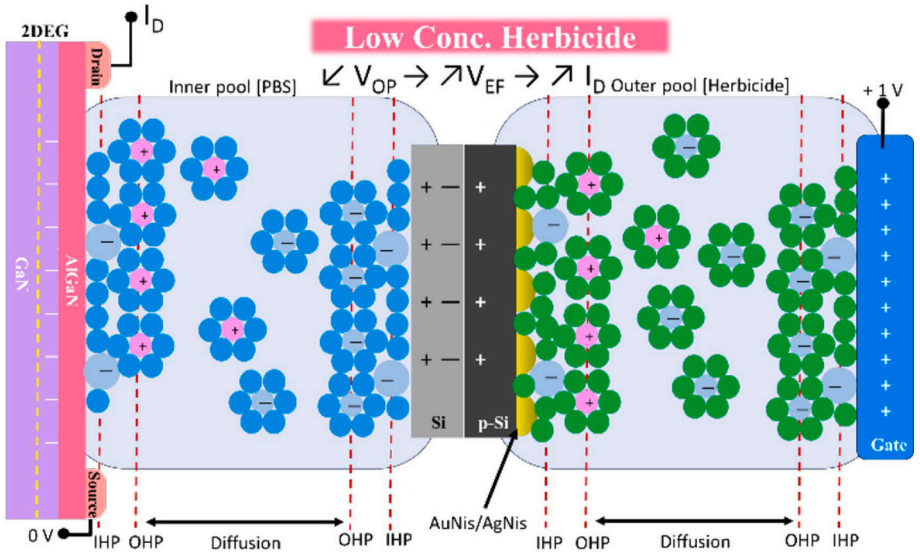

Fig. 3. a) The 2DEG channel in WGHEMT b) The electron concentration (cm^{-3}) and c) The electron current density (A/cm^2) of the 2DEG channel for low and high herbicide concentration.

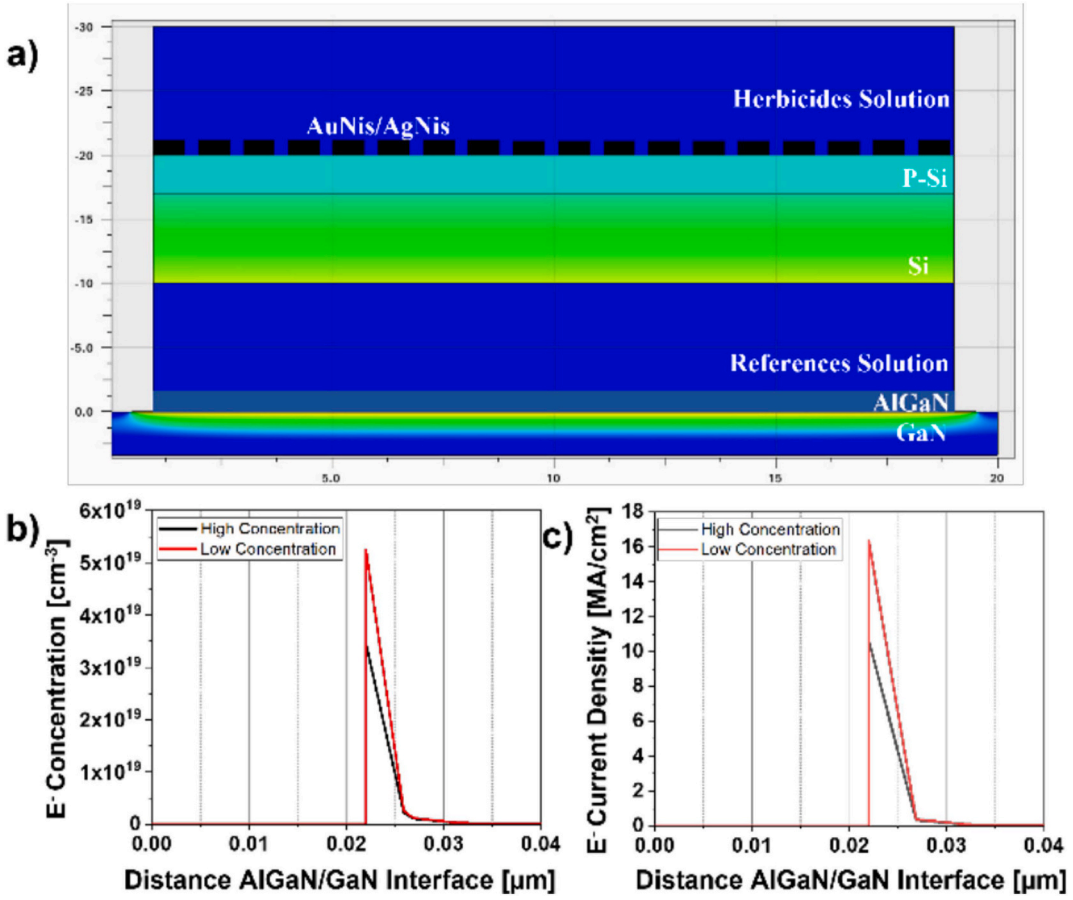

Fig. 4. WGHEMT sensing mechanism in low concentration herbicides.

maintain electrostatic equilibrium. This promotes hole repulsion from the p-Si into the undoped Si region, causing hole accumulation near the undoped Si surface connected to the reference pool, which then attracts additional anions to the OHP. As a result, the value of V_{EF} increases due to the higher overall surface charge caused by the elevated ion density in the OHP. A similar ion balancing process occurs at the AlGaN surface, where the interplay of ions regulates the reference pool's charge distribution. Across the pH range, these ion dynamics enhance the formation of a 2DEG at the AlGaN/GaN interface, thereby contributing to the observed increase in I_D as the pH value rises [31]. The pH current sensitivity and linearity of the WGHEMT device were evaluated based on the linear relationship between I_D and pH at a constant V_D of 1 V, as

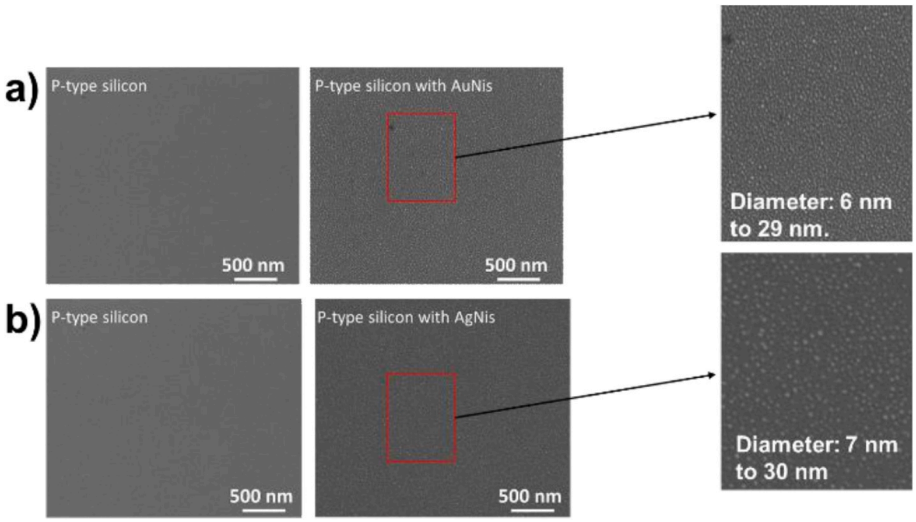

Fig. 5. Uniform and Densely Distributed (a) Gold Nanostructured Islands (AuNis) (b) Silver Nanostructured Islands.

illustrated in Fig. 6b. The device exhibited a current sensitivity of 244.24 μA/pH with a high linearity of $R^2 = 0.9918$. The transfer characteristics, representing I_D as a function of gate voltage (V_G), are shown in Fig. 6c for pH values ranging from 2 to 12, measured at $V_D = 1$ V. A progressive leftward shift in the transfer curve was observed with increasing pH, corresponding to a decrease in the threshold voltage (V_{TH}). The extracted voltage sensitivity was 38.79 mV/pH, with a linearity of $R^2 = 0.94749$, as depicted in Fig. 6d.

WGHEMT current sensitivity and linearity

The electrical response of the WGHEMT sensor exhibits distinct trends in sensitivity and linearity across different herbicide types and formulations, offering valuable insights into its performance. As the concentration of the herbicides increases resulting in a decrease in V_{EF} thus effect the 2DEG. At a concentration of 0.01 mg L^{-1}, the I_D at a V_D of 3 V is 13.97 mA, whereas at 100 mg L^{-1}, I_D drops to 13.75 mA. These results support the proposed WGHEMT sensing mechanism. The stock formulation showed moderate sensitivity (52.00 μA/mg L^{-1}) with good linearity ($R^2 = 0.94879$), consistent with its observed net positive charge behaviour under the test conditions as shown in Figs. 7a and 7b. In contrast, the commercial glyphosate formulation demonstrated a significantly enhanced sensitivity of 222.22 μA/mg L^{-1} and maintained strong linearity ($R^2 = 0.91585$) (see Figures 7c and 7d). This improved performance may be attributed to the presence of surfactants or additives in the commercial product that enhances ionic mobility or promote stronger adsorption at the ISM interface (see).

For paraquat, the stock version exhibited high sensitivity (66.45 μA/

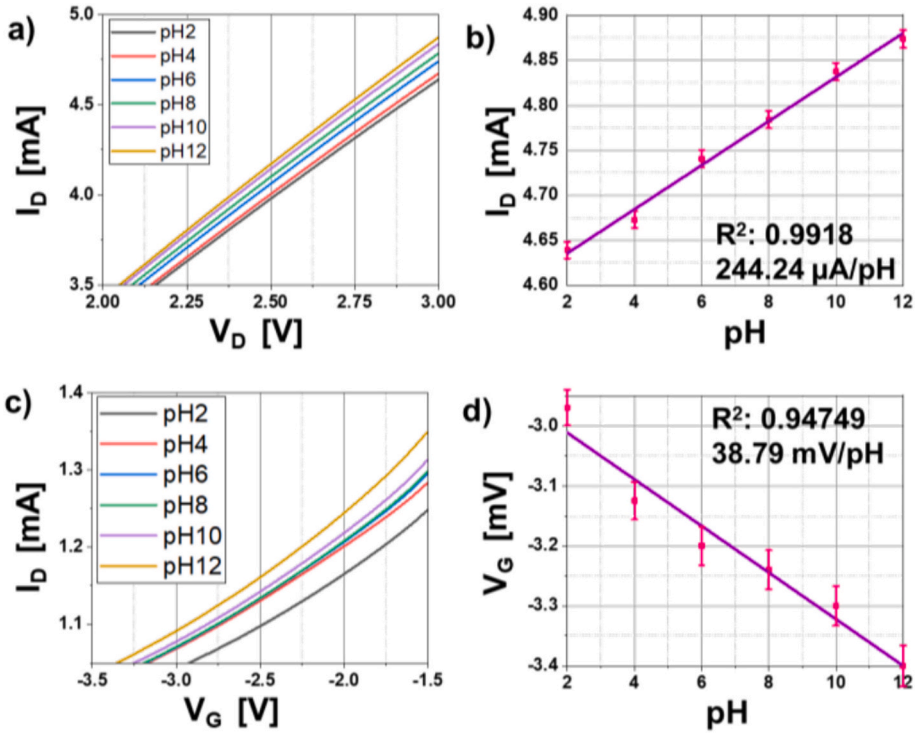

Fig. 6. The graph of (a) the I_D-V_D curve, (b) the current sensitivity and linearity, (c) the I_D-V_G curve, and (d) the voltage sensitivity and linearity with varying pH values.

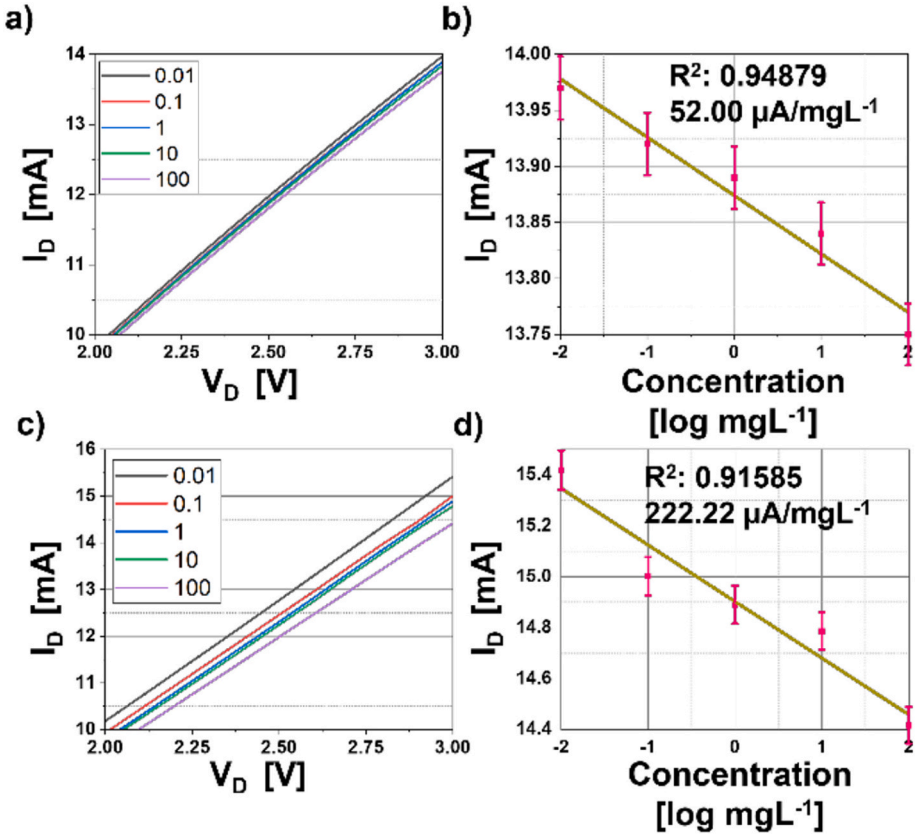

Fig. 7. The graph of (a) the I_D-V_D curve stock glyphosate, (b) the current sensitivity and linearity with of stock glyphosate (c) the I_D-V_D curve commercial glyphosate, and (d) the current sensitivity and linearity with of commercial glyphosate.

mg L^{-1}) but with a linearity (R^2 = 0.92586), indicating strong charge interaction (see Figs. 8a and b. Surprisingly, the commercial paraquat formulation evident in Figs. 8c and 8d showed an even greater sensitivity of 761.029 μA/mg L^{-1}, the highest among all tested herbicides, while also improving linearity (R^2 = 0.96173). This remarkable enhancement suggests that additives in the commercial formulation may

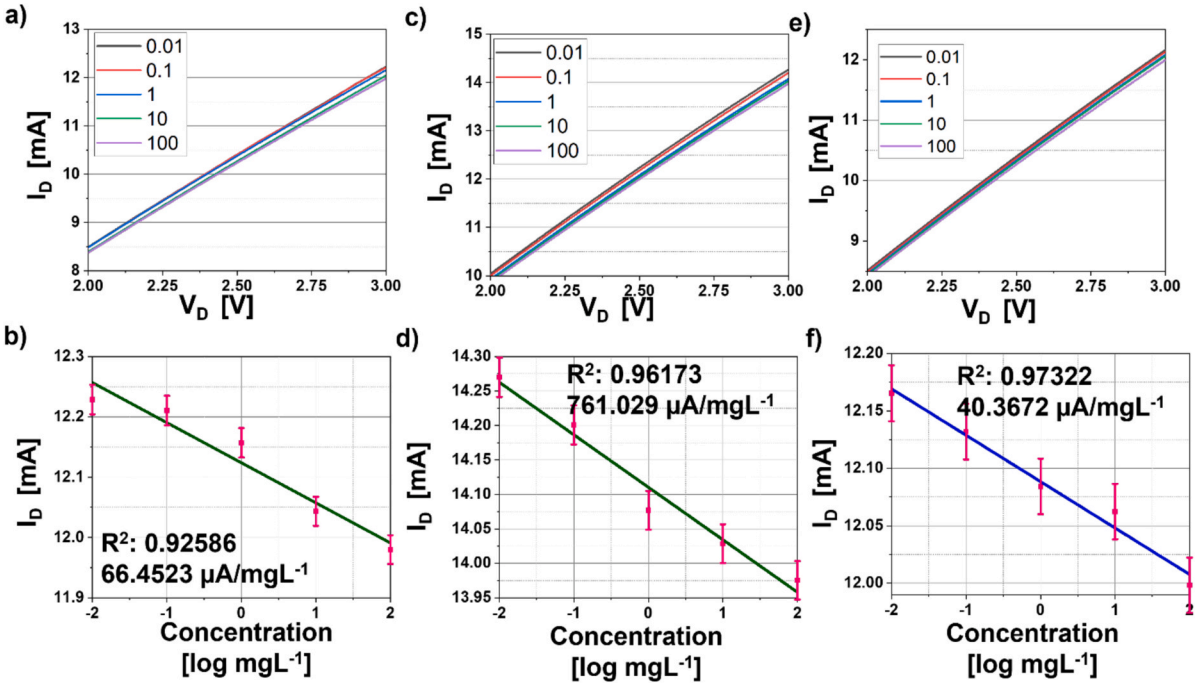

Fig. 8. The graphs of (a) the I_D-V_D curve stock paraquat, (b) the current sensitivity and linearity with of stock paraquat (c) the I_D-V_D curve commercial paraquat, (d) the current sensitivity and linearity with of commercial paraquat, (e) the I_D-V_D curve stock diquat, and (f) the current sensitivity and linearity with of stock diquat.

significantly increase charge availability or facilitate more efficient charge transfer at the sensing interface. As for diquat, which was only available in its stock form due to regulatory restrictions on its commercial use in Malaysia, it showed the best linearity among all tested herbicides ($R^2 = 0.97322$) but the lowest sensitivity (40.37 μA/mg L^{-1}) as seen in Figs. 8e and 8f. This indicates a more uniform yet weaker interaction with the sensing surface, likely influenced by its molecular structure and interaction dynamics under the test conditions. These findings highlight the critical role of analyte charge states, molecular characteristics, and formulation additives in modulating the WGHEMT's electrical response. The results emphasize the importance of calibrating WGHEMTs based on commercial formulations rather than relying solely on pure analytical standards and suggest that optimizing the ISM and surface charge environment is essential for achieving high sensitivity and selectivity in real-world herbicide detection scenarios.

WGHEMT voltage sensitivity and linearity

The potentiometric response of the WGHEMT sensor was evaluated for both stock and commercial herbicide solutions, revealing significant variations in sensitivity and linearity depending on the analyte and formulation. As the concentration of the herbicide increase, the V_{EF} decrease, leading to a reduction in the 2DEG carrier concentration. For glyphosate, the stock formulation exhibited the lowest sensitivity among the tested herbicides at 60 mV/mg L^{-1} and moderate linearity ($R^2 = 0.8896$), likely due to its weaker net charge interaction in its pure analytical form (see Figs. 9a and 9b. In contrast, the commercial glyphosate formulation in Figs. 9c and d showed a substantial improvement, with a sensitivity of 310 mV/mg L^{-1} and slightly lower linearity ($R^2 = 0.8488$). This enhanced performance is attributed to the presence of formulation additives that may increase electrochemical activity or facilitate more effective ion exchange at the ISM interface.

For paraquat, the stock version seen in Figs. 10a and 10b demonstrated a higher sensitivity of 151 mV/mg L^{-1} with good linearity ($R^2 = 0.92709$), reflecting strong and stable charge interactions enabled by its permanent dicationic structure. The commercial paraquat formulation further elevated the WGHEMT response apparent in Figs. 10c and 10d, showing the highest overall sensitivity of 438 mV/mg L^{-1} and excellent linearity ($R^2 = 0.98176$). This result suggests that additional ingredients in the commercial product may enhance charge transfer dynamics and promote stronger interaction with the sensing surface. As for diquat, which was only tested in its stock form due to regulatory restrictions on commercial availability in Malaysia, it showed the highest sensitivity among the stock herbicides at 227.5 mV/mg L^{-1} along with excellent linearity ($R^2 = 0.97137$) as shown in Figs. 10e and 10f. This indicates consistent and effective electrostatic interaction with the WGHEMT sensor, likely due to its molecular configuration and interaction behaviour at the sensing interface. These findings underscore the significant impact of both molecular charge characteristics and commercial formulation components on potentiometric sensor performance. Therefore, for practical herbicide monitoring, sensor calibration should be based on commercial formulations to ensure accuracy and real-world applicability.

WGHEMT reliability and stability

The drift behaviour of the WGHEMT herbicide sensor, represented by the time-dependent I_D in Fig. 11, demonstrates stable and consistent performance. I_D was continuously monitored over a 4-minute period in herbicide solutions with concentrations of 0.01, 0.1, 1, 10, and 100 (mg L^{-1}), revealing minimal signal drift. Across all concentrations, the WGHEMT maintained a drift of less than 1 %, indicating excellent operational stability and reliability. These results confirm the WGHEMT's potential for repeated, real-time monitoring applications.

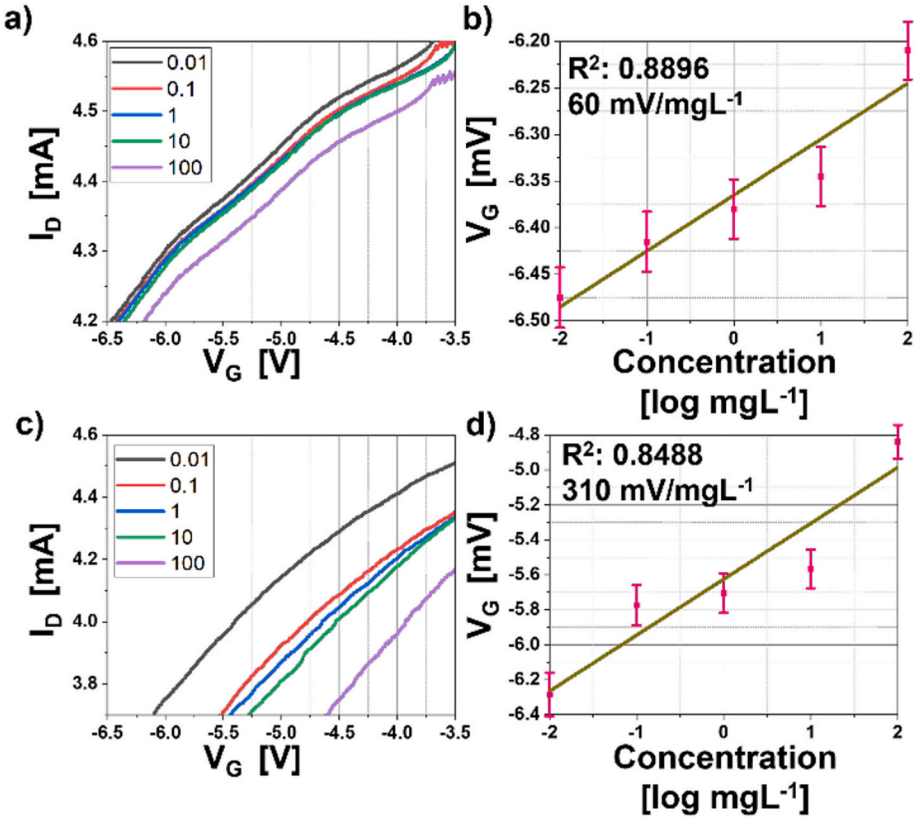

Fig. 9. The graph of (a) the I_D-V_G curve stock glyphosate, (b) the voltage sensitivity and linearity with of stock glyphosate (c) the I_D-V_G curve commercial glyphosate, and (d) the voltage sensitivity and linearity with of commercial glyphosate.

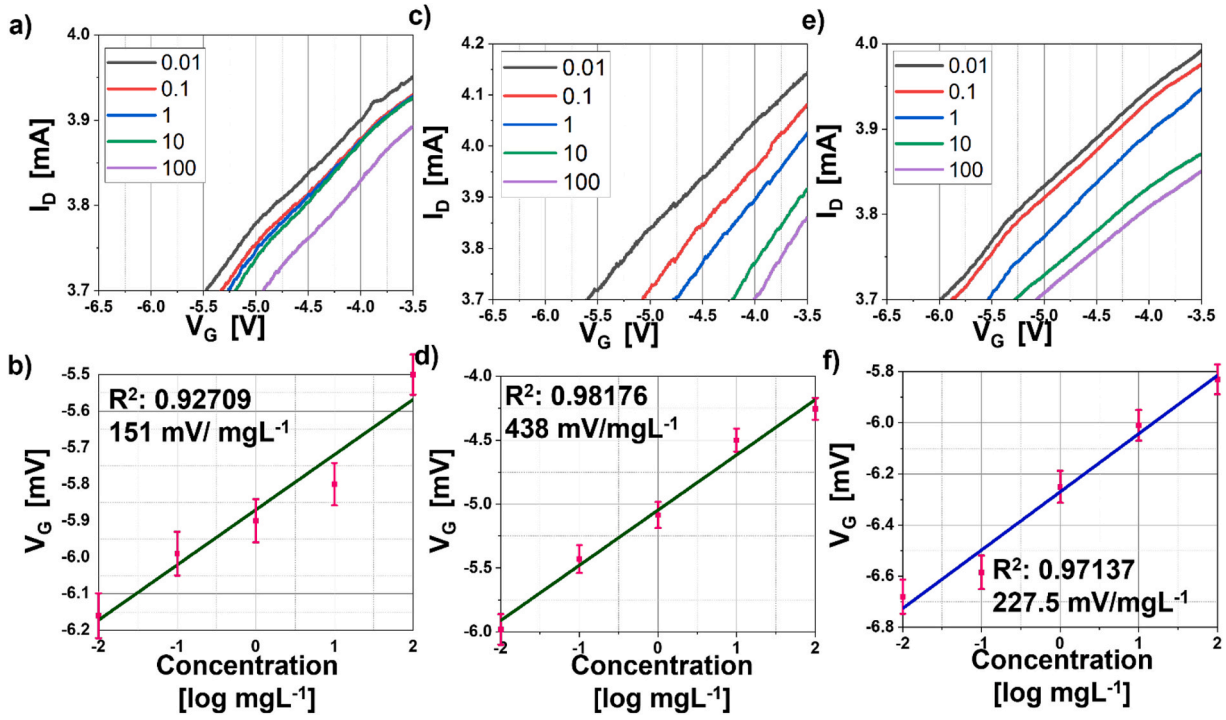

Fig. 10. The graphs of (a) the I_D-V_G curve stock paraquat, (b) the voltage sensitivity and linearity with of stock paraquat (c) the I_D-V_G curve commercial paraquat, (d) the voltage sensitivity and linearity with of commercial paraquat, (e) the I_D-V_G curve stock diquat, and (f) the voltage sensitivity and linearity with of stock diquat.

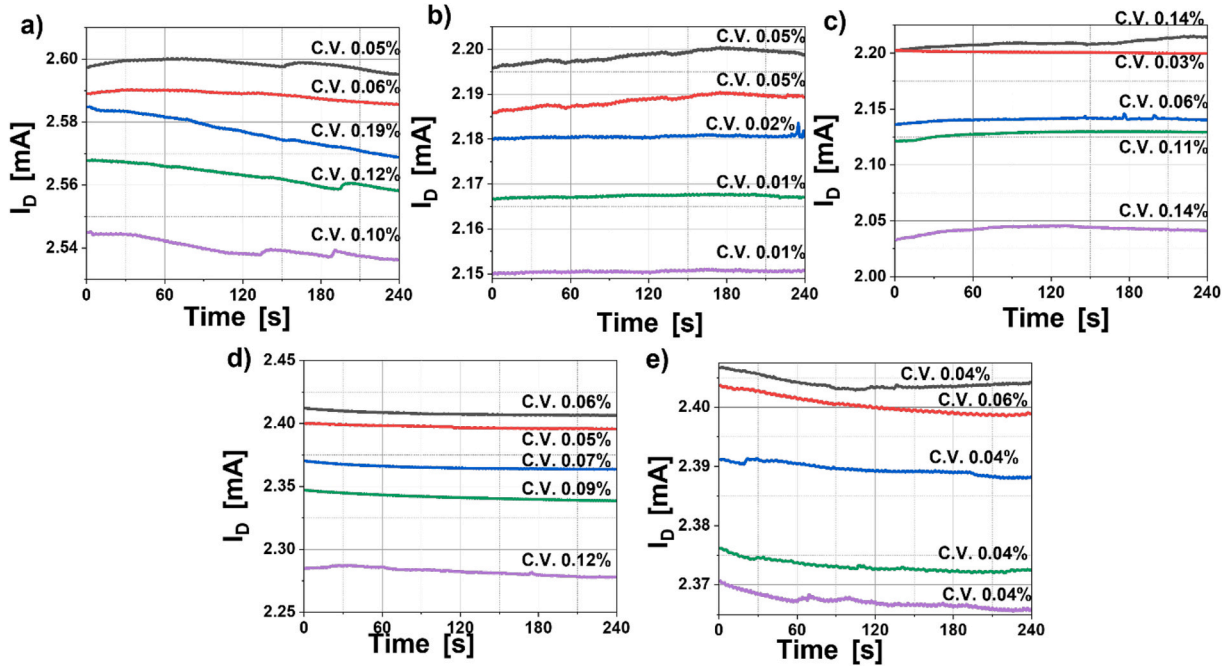

Fig. 11. Reliability and stability test, a) stock glyphosate, b) stock paraquat, c) stock diquat, d) commercial glyphosate, e) commercial paraquat.

Although this evaluation primarily focused on the degradation of maximum I_D over time, other essential performance metrics such as sensitivity, linearity, and repeatability were not assessed in this stability test. Nevertheless, the use of a replaceable ISM in the water-gated configuration may mitigate performance deterioration, suggesting that other parameters are unlikely to degrade at the same rate as $I_{D\ max}$. Further studies are warranted to comprehensively assess long-term stability. Overall, the device demonstrates outstanding stability, and reliability, with variations remaining below 1 %, supporting its compelling capability for herbicide detection applications [43].

Comparative analysis and prospects

These findings establish a strong proof-of-concept for the WGHEMT sensing platform in detecting both stock and commercial herbicide formulations. This work lays a solid foundation for future studies involving real environmental water samples to further assess the sensor's anti-interference capability and real-world applicability. Table 1

Table 1
Comparison of herbicide detection performance between WGHEMT and previously reported sensors.

Water-gated based device	Target analyte	Current sensitivity	Voltage sensitivity	Linear range	Inter-changeable ISM	Stability	Ref
Copper Oxide	Glyphosate	1.72 nA/μM	N/A	5 μmol/L – 15 μmol/L	No	>1 %	[7]
Copper Oxide	Glyphosate	3.00 nA/μM	N/A	5 μmol/L – 15 μmol/L	No	>1 %	[7]
P3CPT	Glyphosate	N/A	N/A	1 μM – 10 μM	No	>1%	[8]
SiO2	Paraquat	N/A	N/A	0.1 nM – 10 μM	No	>1 %	[9]
ZnO/PAC	Diquat	N/A	N/A	0.1 nM – 0.14 μM	No	>1 %	[10]
WGHEMT	Glyphosate	52.00 μA/mg L^{-1}	60 mV/mg L^{-1}	0.01 mg L^{-1} – 100 mg L^{-1}	Yes	<1 %	This work
	Paraquat	66.45 μA/mg L^{-1}	151 mV/mg L^{-1}				
	Diquat	40.37 μA/mg L^{-1}	227.5 mV/mg L^{-1}				
WGHEMT	Commercialise	222.22 μA/mg L^{-1}	310 mV/mg L^{-1}	0.01 mg L^{-1} – 100 mg L^{-1}	Yes	<1 %	This work
	−Glyphosate	761.029 μA/mg L^{-1}	438 mV/mg L^{-1}				
	−Paraquat						

summarizes the herbicide detection results and provides a comparison with other reported sensors. Furthermore, the water-gated configuration combined with an interchangeable ISM sensor provides high current sensitivity for multiple herbicide detection, outperforming other water-gated FET sensors and thereby validating the effectiveness of the proposed system. All measurements were performed using a single HEMT transducer to detect the three herbicides, highlighting the cost-efficiency and versatility of the sensing platform. The high sensitivity and linearity of the WGHEMT are attributed to the gold and silver nanostructured islands, which significantly increase the effective sensing surface area and enhance ion adsorption. The chosen linear detection range of 0.01 mg L^{-1} to 100 mg L^{-1} encompasses realistic herbicide concentrations, with 5.3 mg L^{-1} selected as a representative midpoint. This allows the sensor to detect both lower and higher concentrations within a single dynamic range. These results highlight the WGHEMT's strong potential for practical herbicide detection in environmental monitoring applications.

Conclusion

In conclusion, the WGHEMT sensor demonstrates strong potential for herbicide detection. Among stock herbicides, paraquat showed the highest sensitivity due to its dicationic nature, while diquat exhibited the best linearity and voltage sensitivity. Glyphosate displayed moderate performance in stock form but showed significant improvement in commercial formulations, likely due to additives enhancing ion interactions at the ISM interface. Commercial herbicides solution generally outperformed stock solutions, emphasizing the need for calibration with real-world samples. The WGHEMT also exhibited excellent stability, with signal drift below 1 % over 4 min period, supporting its reliability for real-time monitoring. Overall, the WGHEMT sensor provides an interchangeable ISM, modular configuration that delivers a stable, sensitive, and responsive platform for practical herbicide detection.

CRediT authorship contribution statement

Amirul Firdaus: Writing – original draft, Visualization, Methodology, Investigation, Formal analysis, Data curation. **Najihah Fauzi:** Writing – original draft, Visualization, Methodology, Investigation, Formal analysis, Data curation. **Shuhadah Ismail:** Visualization, Methodology, Investigation, Formal analysis. **Nur Atiqah Hamzah:** Investigation, Formal analysis. **Rashidah Shukor:** Writing – review & editing, Validation, Methodology. **Hiroshi Kawarada:** Writing – review & editing, Validation, Conceptualization. **Shaili Falina:** Writing – review & editing, Writing – original draft, Visualization, Validation, Supervision, Software, Resources, Project administration, Methodology, Investigation, Funding acquisition, Formal analysis, Data curation. **Mohd Syamsul:** Writing – review & editing, Writing – original draft, Visualization, Validation, Supervision, Software, Resources, Project administration, Methodology, Investigation, Funding acquisition, Formal analysis, Data curation, Conceptualization.

Declaration of competing interest

The authors declare that they have no known competing financial interests or personal relationships that could have appeared to influence the work reported in this paper.

Acknowledgements

The authors gratefully acknowledge the Ministry of Higher Education Malaysia for funding this project through the Higher Institution Centre of Excellence (HICoE) program, under the Institute of Nano Optoelectronics Research and Technology (INOR), with Project Code: A305-KR-AKH002-0000000434-K134. The authors would like to express their sincere appreciation to Zhao Haocheng for performing the simulation work to validate the findings of this study.

Data availability

Data will be made available on request.

References

[1] Van Bruggen AHC, et al. Environmental and health effects of the herbicide glyphosate. Sci Total Environ 2018;616–617:255–68. https://doi.org/10.1016/j.scitotenv.2017.10.309.
[2] Ali C, Patrick C, Thierry B. Corps étranger de l'urètre et dépression mélancolique, les implications diagnostiques aux urgences - à propos d'un cas clinique. Pan Afr Med J 2011;9:1–5.
[3] Benbrook CM. Trends in glyphosate herbicide use in the United States and globally. Environ Sci Eur 2016;28(1):1–15. https://doi.org/10.1186/s12302-016-0070-0.
[4] Battaglin WA, Meyer MT, Kuivila KM, Dietze JE. Glyphosate and its degradation product AMPA occur frequently and widely in U.S. soils, surface water, groundwater, and precipitation. J Am Water Resour Assoc 2014;50(2):275–90. https://doi.org/10.1111/jawr.12159.
[5] Dinis-Oliveira RJ, Duarte JA, Sánchez-Navarro A, Remião F, Bastos ML, Carvalho F. Paraquat poisonings: mechanisms of lung toxicity, clinical features, and treatment. Crit Rev Toxicol 2008;38(1):13–71. https://doi.org/10.1080/10408440701669959.
[6] Suntres ZE. Role of antioxidants in paraquat toxicity. Toxicology 2002;180(1):65–77. https://doi.org/10.1016/S0300-483X(02)00382-7.
[7] Ogurcovs A, Kadiwala K, Sledevskis E, Krasovska M, Mizers V. Glyphosate sensor based on nanostructured water-gated CuO field-effect transistor. Sensors 2022;22(22):1–14. https://doi.org/10.3390/s22228744.
[8] Asano K, et al. Real-time detection of glyphosate by a water-gated organic field-effect transistor with a microfluidic chamber. Langmuir 2021;37(24):7305–11. https://doi.org/10.1021/acs.langmuir.1c00511.
[9] Wang H, Guo J, Chen Y, Xu N, Xu T, Xu Z. Highly sensitive paraquat sensor based on Ag@TiO2/MXene functionalized solution-gate graphene field-effect transistor. Microchem J 2025;212(March). https://doi.org/10.1016/j.microc.2025.113362.
[10] Sain Tanwar A, Mehtab M, Kim JT, Oh KJ, Krishnan Iyer P, Im YH. Real-time selective pesticide detection using catalytic behavior of zwitterionic conjugated polymer. Chem Eng J 2023;456(July 2022):141002. https://doi.org/10.1016/j.cej.2022.141002.
[11] Tu A, Muddiman DC. Systematic evaluation of repeatability of IR-MALDESI-MS and normalization strategies for correcting the analytical variation and improving image quality. Anal Bioanal Chem 2019;411(22):5729–43. https://doi.org/10.1007/s00216-019-01953-5.
[12] Kolosova AY, Shim WB, Yang ZY, Eremin SA, Chung DH. Direct competitive ELISA based on a monoclonal antibody for detection of aflatoxin B1. Stabilization of ELISA kit components and application to grain samples. Anal Bioanal Chem 2006;384(1):286–94. https://doi.org/10.1007/s00216-005-0103-9.

[13] Pérez-Fernández B, Costa-García A, De La Escosura-Muñiz A. Electrochemical (bio) sensors for pesticides detection using screen-printed electrodes. Biosensors 2020; 10(4). https://doi.org/10.3390/bios10040032.
[14] Vu CA, Chen WY. Field-effect transistor biosensors for biomedical applications: recent advances and future prospects. Sensors (Switzerland) 2019;19(19). https://doi.org/10.3390/s19194214.
[15] Berto M, et al. Label free detection of plant viruses with organic transistor biosensors. Sensors Actuators, B Chem 2018;281(October 2018):150–6. https://doi.org/10.1016/j.snb.2018.10.080.
[16] Paolucci F, et al. Electrostatic field-driven supercurrent suppression in ionic-gated metallic superconducting nanotransistors. Nano Lett 2021;21(24):10309–14. https://doi.org/10.1021/acs.nanolett.1c03481.
[17] Ambacher O, et al. Two-dimensional electron gases induced by spontaneous and piezoelectric polarization charges in N- and Ga-face AlGaN/GaN heterostructures. J Appl Phys 1999;85(6):3222–33. https://doi.org/10.1063/1.369664.
[18] Umesh Y-FW, Mishra K, Fellow IEEE, Shen L, Kazior TE. GaN-based RF power devices and amplifiers. Encycl Mater Sci Technol 2001;96(2):1118–22. https://doi.org/10.1016/b0-08-043152-6/00209-6.
[19] Anvari R, Spagnoli D, Umana-Membreno GA, Parish G, Nener B. Effect of pH and structure on the channel conductivity of AlGaN/GaN heterostructure based sensors. Sensors Actuators, B Chem 2018;269:54–61. https://doi.org/10.1016/j.snb.2018.04.148.
[20] Hu S, et al. A miniature biomedical sensor for rapid detection of schistosoma japonicum antibodies. Biosensors Aug. 2023;13(8):831. https://doi.org/10.3390/bios13080831.
[21] Kergoat L, et al. A water-gate organic field-effect transistor. Adv Mater 2010;22 (23):2565–9. https://doi.org/10.1002/adma.200904163.
[22] Sriramani P, Mohankumar N, Durai L, Prasamsha Y, Rakesh N. Analytical model for DG-AlGaN/GaN MOS-HEMT for sensitive analysis of pH analytes and charged biomolecules. Sensors Int 2025;6(July 2024):100312. https://doi.org/10.1016/j.sintl.2024.100312.
[23] Pouthas F, Gentil C, Côte D, Bockelmann U. DNA detection on transistor arrays following mutation-specific enzymatic amplification. Appl Phys Lett 2004;84(9): 1594–6. https://doi.org/10.1063/1.1650907.
[24] Schmoltner K, Kofler J, Klug A, List-Kratochvil EJW. Electrolyte-gated organic field-effect transistor for selective reversible ion detection. Adv Mater 2013;25(47): 6895–9. https://doi.org/10.1002/adma.201303281.
[25] Ding J, Qin W. Recent advances in potentiometric biosensors. TrAC - Trends Anal Chem 2020;124:115803. https://doi.org/10.1016/j.trac.2019.115803.
[26] Alghamdi N, Alqahtani Z, Grell M. Sub-nanomolar detection of cesium with water-gated transistor. J Appl Phys 2019;126(6):Aug. https://doi.org/10.1063/1.5108730.
[27] Alqahtani Z, Alghamdi N, Grell M. Monitoring the lead-and-copper rule with a water-gated field effect transistor. J Water Health Apr. 2020;18(2):159–71. https://doi.org/10.2166/wh.2020.186.
[28] Liao C, Mak C, Zhang M, Chan HLW, Yan F. Flexible organic electrochemical transistors for highly selective enzyme biosensors and used for saliva testing. Adv Mater 2015;27(4):676–81. https://doi.org/10.1002/adma.201404378.
[29] Firdaus A, Fauzi N, Ismail S, Kawarada H, Falina S, Syamsul M. Advanced potentiometric configuration to enhance stability and reliability of AlGaN/GaN HEMT-based water-gated pH sensor. J Electrochem Soc 2024;171(8):087513. https://doi.org/10.1149/1945-7111/ad6e21.
[30] Do MH, et al. Chitosan-based nanocomposites for glyphosate detection using surface plasmon resonance sensor. Sensors (Switzerland) 2020;20(20):1–19. https://doi.org/10.3390/s20205942.
[31] Duan B, Yang L, Wang Y, Yang Y. Experimental results for AlGaN/GaN HEMTs improving breakdown voltage and output current by electric field modulation. IEEE Trans Electron Devices 2021;68(5):2240–5. https://doi.org/10.1109/TED.2021.3067865.
[32] Ali S, et al. A facile approach based on functionalized silver nanoparticles as a chemosensor for the detection of Paraquat. J Clust Sci 2022;33(1):413–20. https://doi.org/10.1007/s10876-021-01978-w.
[33] Hu P, et al. A SERS-based point-of-care testing approach for efficient determination of diquat and paraquat residues using a flexible silver flower-coated melamine sponge. Food Chem 2024;454(February):139831. https://doi.org/10.1016/j.foodchem.2024.139831.
[34] Allagui A, Benaoum H, Olendski O. On the Gouy–Chapman–Stern model of the electrical double-layer structure with a generalized Boltzmann factor. Phys A Stat Mech Its Appl 2021;582:126252. https://doi.org/10.1016/j.physa.2021.126252.
[35] Kim S, Seo J, Choi J, Yoo H. Vertically integrated electronics: new opportunities from emerging materials and devices. Nano-Micro Lett 2022;14(1):1–29. https://doi.org/10.1007/s40820-022-00942-1.
[36] Ciampi S, Darwish N, Aitken HM, Díez-Pérez I, Coote ML. Harnessing electrostatic catalysis in single molecule, electrochemical and chemical systems: a rapidly growing experimental tool box. Chem Soc Rev 2018;47(14):5146–64. https://doi.org/10.1039/C8CS00352A.
[37] A. Varghese, P. Das, and S. Tallur, "A Complete Analytical Model for MOS-HEMT Biosensors: Capturing the Effect of Stern Layer and Charge Screening on Sensor Performance," *IEEE Sensors Lett.*, vol. 5, no. 4, 2021, doi: 10.1109/LSENS.2021.3065509.
[38] Meddeb-Limem S, Ben Fredj A. Computational study of the dimerization of glyphosate: mechanism and effect of solvent. RSC Adv 2024;14(32):23184–203. https://doi.org/10.1039/d4ra04300f.
[39] Pérez-Chávez NA, Albesa AG, Longo GS. Molecular theory of glyphosate adsorption to pH-responsive polymer layers. Adsorption 2019;25(7):1307–16. https://doi.org/10.1007/s10450-019-00091-9.
[40] Borggaard OK, Gimsing AL. Fate of glyphosate in soil and the possibility of leaching to ground and surface waters: a review. Pest Manag Sci 2008;64(4): 441–56. https://doi.org/10.1002/ps.1512.
[41] Groß A, Sakong S. Modelling the electric double layer at electrode/electrolyte interfaces. Curr Opin Electrochem 2019;14:1–6. https://doi.org/10.1016/j.coelec.2018.09.005.
[42] Yaseen M, et al., of Nanostructured Gold : A Critical Review, pp. 1–83, 2021.
[43] Slewa LH, Abbas TA, Ahmed NM. Synthesis of quantum dot porous silicon as extended gate field effect transistor (EGFET)for a pH sensor application. Mater Sci Semicond Process 2019;100(April):167–74. https://doi.org/10.1016/j.mssp.2019.04.045.